IEEE Access
Multidisciplinary | Rapid Review | Open Access Journal

Received August 12, 2020, accepted August 28, 2020, date of publication September 1, 2020, date of current version September 18, 2020.

Digital Object Identifier 10.1109/ACCESS.2020.3021003

Dielectric Performance of Magneto-Nanofluids for Advancing Oil-Immersed Power Transformer

MD RASHID HUSSAIN[1], (Graduate Student Member, IEEE),
QASIM KHAN[2], (Graduate Student Member, IEEE),
ASFAR ALI KHAN[3], (Member, IEEE),
SHADY S. REFAAT[1], (Senior Member, IEEE),
AND HAITHAM ABU-RUB[1], (Fellow, IEEE)

[1]Department of Electrical and Computer Engineering, Texas A&M University, Doha, Qatar
[2]Department of Electrical and Computer Engineering, Texas A&M University, College Station, TX 77843, USA
[3]Department of Electrical Engineering, Aligarh Muslim University, Aligarh 202002, India

Corresponding author: Md Rashid Hussain (md_rashid.hussain@qatar.tamu.edu)

This work was supported by the Qatar National Research Fund (a member of the Qatar Foundation) under Grant 10-0101-170085, and the High Voltage Engineering Laboratory, AMU, Aligarh, India. Open Access funding provided by the Qatar National Library.

ABSTRACT Recently, nanofluids are introduced in the power utilities for the dielectric performance enhancement of power transformer oil. The compactness and fault improvement of the power transformers has resulted in the necessity of next-generation insulating fluid with inflated dielectric properties. This article investigates the dielectric performance of the novel ester oil-based magnetic nanofluids with different nanoparticles under different electric stress conditions. Two biodegradable fluids used as the base liquid for the experiment are synthetic ester oil and natural ester oil while three magnetic nanoparticles used to synthesize nanofluids are iron (II, III) oxide, cobalt (II, III) oxide, and iron phosphide. The concentrations of the nanoparticles are varied to optimize the characteristics of the prepared nanofluids. The dielectric breakdown and relative permittivity of the nanofluids have been experimentally investigated. Further, the breakdown predictions have been performed using Weibull statistical distribution-based regression analysis. The experimental results show the improvement in the characteristics of prepared nanofluids with the change in nanoparticle concentration as compared with the host fluids.

INDEX TERMS Magnetic nanofluids, transformer oil, breakdown characteristics, Weibull distribution, relative permittivity, Ester oil.

I. INTRODUCTION

The power transformer is the heart of the electric power system due to vast applicabilities in the generation, transmission, and distribution levels. The reliable and efficient operation of the electrical power transformer significantly depends on its insulation characteristics, as it constitutes the major portion of the transformer failure. The insulating oil plays a crucial role in the power transformer lifespan as it performs both the insulation as well as the coolant functionality [1]. The electrical power transformers during its operating life are exposed to a variety of stresses, such as mechanical, thermal, electrical, and environmental stresses. The advancement in power transformer comprises the objective of better electrical and thermal insulation with minimum liquid insulation quantity to diminish the transformer size [2]. The insulating material must be able to withstand different stresses to prevent short circuits and leakage currents. The conventional insulating oils are incapable to fulfill the compactness requirement and face many faults with growing stresses. Therefore, new liquid insulation or some additional supporting reagents are required with conventional oil should be developed to meet all demands of the futuristic power transformer. Consequently, the evolution of nanotechnology in the power area is an essential step towards improvement in liquid dielectrics [3]. Nanotechnology is flourishing rapidly due to the demand

The associate editor coordinating the review of this manuscript and approving it for publication was Nagarajan Raghavan.

for improved quality of insulating oil and has become an important part of the research.

The word 'Nanofluid' was coined by Dr. Stephen Choi in the year 1993, where the nano-scaled sized particles-based coolant was prepared for achieving improved stability and thermal conductivity [4], [5]. Nanofluids (NFs) are described as the colloidal suspension of nanoparticles (NPs) with the size between 1 to 100 nm evenly dispersed in the insulating medium which can be created either by chemical or physical processes [6]. It has anomalous physical, and thermal transport properties. The small size of particles support to deliver a stable suspension, better thermal conductivity, reduced physical erosion, and lower pumping power. The addition of a very little amount of NPs into the insulating medium shows a noteworthy alteration in the electrical and thermal properties [7]. The improvement due to NPs relies on the numerous physical, chemical, and thermal characteristics of NPs along with the base medium. The enhanced heat transfer capability and electrical property have resulted in the exploration of NFs to a vast extent, especially as the alternative for transformer oil.

Magneto-Nanofluids (ferrofluids) contain evenly distributed NPs-based fluid which use magnetic NPs to achieve superior dielectric property for transformer oil [8]. Recently, many types of research have been carried out on magneto-NFs that show promising dielectric and thermal properties as transformer oil [9]–[11]. Lv *et al.* [9] proposed the magnetic NFs suitable for high voltage insulation by verifying improved dielectric strength with NP concentration. Rafiq *et al.* [10] illustrated an improvement with ac and impulse breakdown strength on magnetic NFs with mineral oil as the base fluid. While Kim and Lee [11], carried out experiments on the breakdown strength of mineral oil-based ferrofluids under the effect of the magnetic field displaying promising results in high voltage applications. The improved thermal and electrical properties of magnetic NFs in transformer windings also elevate the switching and lightning impulse withstand capability of power transformer with the insignificant impact of the moisture [12].

Several research papers in the breakdown of NFs have been published in the present years. Danikas *et al.* [13] performed some experimental work related to the breakdown characteristics of natural ester oil and mineral oil. The breakdown voltages of prepared NFs have been observed to be higher when compared to the host oil. Table 1 shows different commercially available liquid insulating materials used in power transformers which are categorized into three main types: mineral insulating oil, synthetic insulating oil, and vegetable insulating oil [14].

Some of the works have been performed in the past regarding the temperature affecting the NFs [15], [16]. In [15], the authors performed the experimental analysis on the A.C breakdown characteristics of host oil and ZrO_2-based NFs considering the effect of temperature. The results carried out during this process were positive, as the higher breakdown strength of NFs compared to host oil at higher temperatures

TABLE 1. Types of insulating oil [14].

Oils	Types	Description
Mineral Oil	Paraffinic oils	long-chained without ring
	Naphthenic oils	Saturated with the ring
	Aromatic oils	Unsaturated ring
Synthetic Oil	Polyalphaolefins	Produced by polymerization of hydrocarbon molecules
	Polyglycols	Manufactured by the oxidation of ethylene and propylene
	Synthetic ester oils	Produced by the treatment of acids and alcohols with water
Vegetable Oil	Soybean oil	decomposable, low inflammable, better dielectric strength, high flash point, high viscosity and pour point
	Coconut oil	
	Cottonseed oil	
	Rapeseed oils	

was evident. The reason for the increase in the breakdown voltage for any fluid is due to the reduction in the relative humidity of oil. For NFs, NPs in the NF have the ability to absorb moisture from the surrounding due to induced relative interfacial polarization creating more robust fluid than host oil [16].

While synthesizing the NFs, the stability of NF is a significant requirement to attain a longer lifespan [17]. The stability of NFs implies the consistent dispersion of NPs in the insulating oil and restrict any settlement or coagulation of NPs during its operating life [18]. The force of attraction among NPs creates particle clusters that later deposit down due to higher density [19]. Therefore, short term stability due to the increasing size of clusters is the obstacle for any NFs to be utilized in practical applications [9]. The limitation can be overcome with the help of stabilizing agents known as surfactants which vary depending on the NPs, base liquid, and applications [19].

The main contribution of this article is to illustrate the dielectric performance of the novel iron phosphide NPs-based NF along with cobalt (II, III) oxide and iron (II, III) oxide-based NF. The effectiveness of the prepared magneto-NFs is determined by the dielectric characteristics and breakdown strength measurement. The determined performance provides the NF applicability as a conventional transformer oil replacement. All these characteristics of the prepared NFs and other NFs have been investigated and discussed. Further, statistical analysis is presented to examine the breakdown probability by the Weibull Distribution regression analysis.

The paper is organized as follows. The experimental work on the dielectric strength of NFs is detailed in Section II. The obtained results of prepared NFs along with the discussion is presented in Section III. The conclusion is provided in Section IV. Section V gives a comprehensive overview of NFs and its characteristic properties.

II. EXPERIMENTAL WORK

To validate the theoretical analysis, a series of experiments were conducted to find the potential of NFs. Firstly, the NPs and dielectric fluids are selected to prepare the NFs based on their properties. The breakdown voltage (BDV) tests are performed for each prepared NFs having different NP concentrations through oil breakdown voltage tester. Further, the relative permittivity of each prepared NFs is measured by the dielectric constant kit. Step by step experimental work is detailed as follows:

A. MATERIALS USED

The magnetic NPs picked for the experimental work are iron phosphide (Fe_3P), cobalt (II, III) oxide, and iron (II, III) oxide. Cobalt (II, III) oxide and iron (II, III) oxide nanoparticles were purchased from Sigma-Aldrich. Whereas, are iron phosphide (Fe_3P) microparticles was purchased from Sigma-Aldrich and further synthesized by top-down nanotechnology approach to form nanopowder [20]. Dielectric fluids taken in the experiment are commercially accessible synthetic ester oil and natural ester oil. For stabilizing the NPs oleic acid is used.

B. PREPARATION

Based on the number of steps, NFs can be manufactured either in a one-step or two-step method [21]. One-step method involves the dispersion and synthesis of NPs that are simultaneous, i.e., the processes of drying, storing, and transference are not practiced and, therefore, results in enhancement and minimization of agglomeration of stable nano-based oil. While two-step process comprises a two-phase method i.e., synthesizing the nanofillers followed by the dispersing of the nanofillers into the host fluid by utilizing mechanical or thermal techniques (such as mechanical agitation, ultrasonication, and magnetic stirring).

The two-step technique reduces the probability of clusters pertaining due to the force of attraction between the NPs, which causes the settling of NPs. However, the coagulation of the NPs could not be completely eliminated without using surfactants. The magnetic NPs are efficiently coated with oleic acid as a surfactant with oil as a base medium to provide better stability in the insulating medium [22].

The surfactants are the stabilizing agents (may or may not be added in the liquid) which are used for the proper distribution of NPs into the solution to minimize the settlement and coagulation of NPs [23]. Fe_3P is a magnetic nature bulky NP that requires stabilizing agents. The two-step method is selected in this experimental work for the synthesis of magnetic NFs as shown in Figure 1. For achieving the active surface of the NPs, 10% concentration of the oleic acid solution (500 ml solution) is intermixed by the application of magnetic stirrer for a period. 10% concentration of the oleic acid solution is taken to be 0% of NP concentration for this experiment. Further, the desired quantity of NPs is added to the prepared solution. NPs concentrations in the scale of milligrams are added to form different NP concentrations

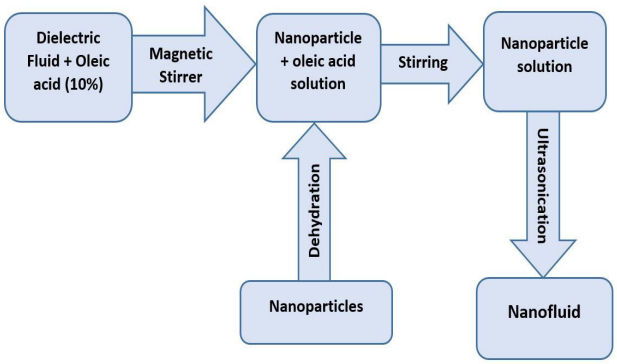

FIGURE 1. Block diagram representation of nanofluid synthesis by the two-step method.

of NFs In this experiment, 0.0012%, 0.0022%, 0.003% and 0.004% of NP solutions are prepared for each type of NP. To disperse the NPs completely into the solution, the solution undergoes the ultra-sonication process, which utilizes sound energy having alternating high and low pressure for the dispersion. Sonication is the process in which the ultrasound waves whose frequency value of 20 kHz (20,000 cycles per second) or higher are used to create the vibrations for the dispersion of NFs. The solution is kept in the ultrasonicator for around 2-3 hours. The sample was changed after every six repetitive breakdowns.

C. ELECTRICAL MEASUREMENT

The performance of any insulating oil can be investigated by some specific set of experimental analyses in the form of withstand breakdown strength, dielectric measurement, etc. Both the measurements have been taken into consideration in this article to investigate and analyze prepared NFs.

The first measurement is the AC breakdown strength of NFs as the transformer functioning is based on the AC voltage source. The dielectric breakdown involves numerous pre-breakdown stages and is observed by the development of an arc which is the electrical short circuit causing a large flow of the current between the electrodes. The BDVs of different NF samples are recorded using the oil breakdown tester as per IEC 60156 with two standardized electrode configurations as shown in Figure 2(a) and 2(b). The standardized electrode configurations i.e., Verband Deutscher Elektrotechniker (VDE) electrode which is a mushroom-shaped electrode, and spherical electrode with specific gaping between them to provide different stresses conditions. According to IEC 60156 standard, the method of dielectric breakdown test is performed by applying an AC test voltage with the help of a step-up transformer. The frequency range of the test voltage should be between 48 Hz to 62 Hz. The voltage supplied to the test sample should be 5 minutes after filling the oil vessel up to the oil level and the air bubbles must not be evident in the electrode gap. The voltage initially at zero, is raised at a rate of 2.0 $kVs^{-1} \pm 0.2$ kVs^{-1} and stopped till the breakdown takes place. Figure 2(c) and 2(d) represents the flashover in the form of visible spark during dielectric

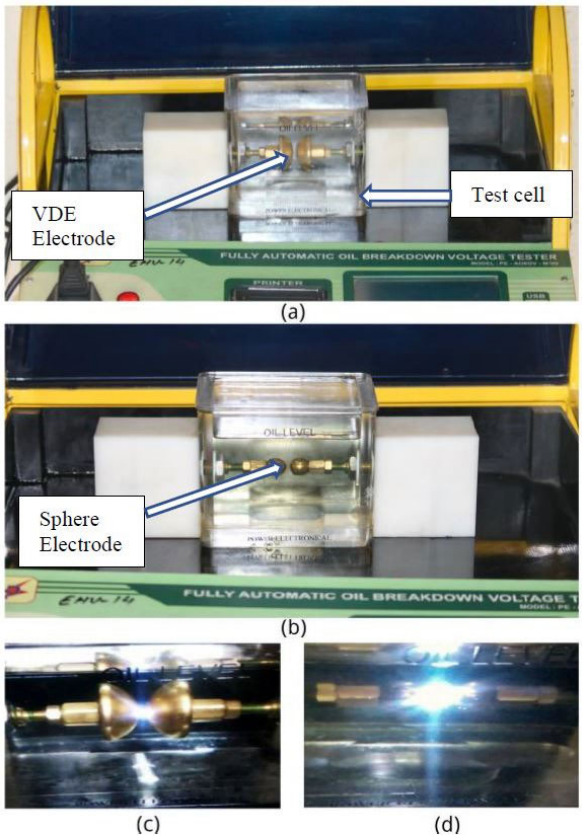

FIGURE 2. Automatic breakdown voltage tester for measuring breakdown voltage of dielectric liquid; (a) VDE electrode configuration; (b) Sphere-Sphere electrode configuration; (c) VDE electrode during dielectric breakdown; (d) Sphere-Sphere electrode configuration during dielectric breakdown.

breakdown. At least two minutes break is maintained in each breakdown test and no gas bubble exists within the electrodes gap before each breakdown measurement. Repetitive breakdowns are measured on each prepared fluid sample where there were no NPs evident on the electrode during or after the breakdown process. The concentration of each type of NPs is kept consistent as much as possible in both base oil to attain uniformity.

The second measurement is the dielectric permittivity of the oil. The relative permittivity of the prepared NFs has been calculated by using the dielectric constant kit and standard oil test cell. The standard dielectric is a capacitance and dissipation factor (Tan δ) bridge which measures relative permittivity based on the ratio of capacitance. The oil cell maintains the uniform air gap at each surface of the electrodes.

III. RESULTS AND DISCUSSION

A. AC BREAKDOWN STRENGTH

The result of the prepared NFs needs to be analyzed to properly observe the dielectric characteristics. Some results of BDV of NFs are taken from author's previuos work [24]. The normalization of breakdown voltage (BDV) is performed by dividing the mean breakdown voltage of NF (BDV_{mean_nf}) to the breakdown voltage of their respected base oil ($BDV_{mean\_base\_oil}$). The enhancement in the breakdown strength needs to be investigated to evaluate the performance of NF with the increase in NP concentration. The percentage enhancement (ΔBDV (%)) is calculated by using the formula as shown in equation (1).

$$\Delta BDV\ (\%) = \left(\frac{BDV_{mean\_nf}}{BDV_{mean\_base\_oil}} - 1 \right) * 100 \qquad (1)$$

The comparative results of all NFs with different electrode configurations are provided in Figure 3. The variation in average breakdown voltage with varying NF concentration are plotted. The mean breakdown voltage (BDV_{mean}) and standard deviation are also significant for repetitive breakdown testing as shown in Figure 3. The percentage breakdown enhancement for each NF at the individual NP concentrations is denoted in the graph accordingly along with the range in the breakdown strength at each point. The electrode system VDE is represented by Mushroom-Mushroom (M-M) electrode system while the sphere-sphere (S-S) electrode system in all figures. As the gap between the M-M electrode is larger than the S-S electrode system which results in higher BDV for the M-M electrode system for each insulating fluid.

Each NF can sustain a specific amount of NP concentration which can be considered its saturation point or critical point. Beyond the saturation point, the addition of NP in the base oil negatively influences its characteristics. The enhancement in the breakdown voltage of the prepared magnetic NF is due to high electron scavenging property of the dispersed nanoparticles during the application of the high voltage. Electron scavenging property of slow moving nanoparticles decrease the rapid motion of electrons, which subdue the streamer formation, and lead to increase in the breakdown strength of the prepared NFs. The variation in normalized BDV for iron phosphide NP-based NFs is shown in Figure 3(a). Fe_3P NPs-based NFs initially show positive enhancement with the addition of up to 0.0022% NP concentration with synthetic ester oil as a base fluid. Beyond this point, the normalized BDV shows a negative enhancement or drop in BDV for NP having the concentrations greater than 0.0022% with synthetic ester as base fluid. It indicates nanoparticles create agglomeration near the electrode developing high electric field resulting in lowering the breakdown voltage of NF. The saturation in the NP is achieved above 0.0022% as shown in Figure 3(a). Breakdown strength is not measured above 0.004%, as BDV drop below base oil BDV.

When the base fluid in NF is changed to natural ester oil, the saturation point goes beyond 0.004% NP as shown in Figure 3(a) in both configurations. Also, Breakdown strength keeps increasing with NP concentration with natural ester oil. Natural ester oil shows more accumulation possibility for NPs as compared to synthetic ester oil resulting in stable dispersion at higher concentration.

Similar trends are shown by iron oxide NPs with synthetic ester oil as a base fluid in NF as shown in Figure 3(b) except that iron phosphide-based NF shows a larger drop as compared with iron oxide-based NF. It is due to similar size and similar magnetic nature of both compounds. Enhancement in

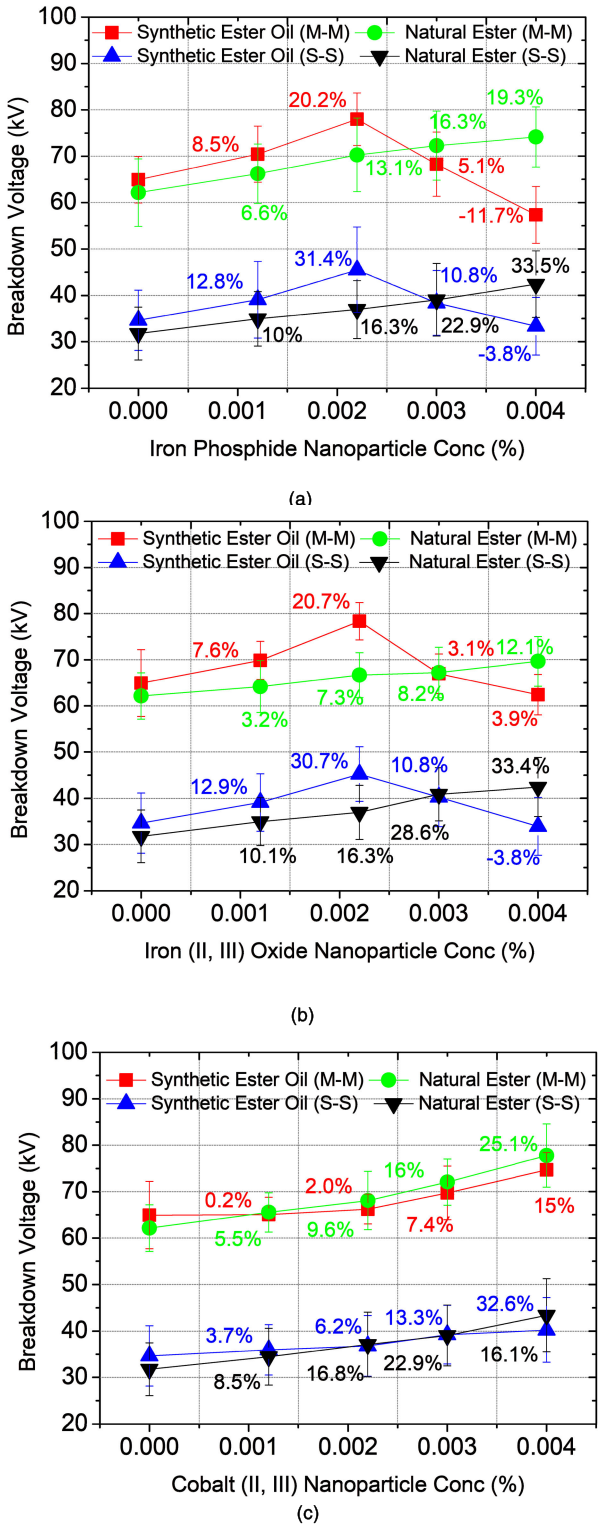

FIGURE 3. The variation in breakdown strength of NFs with respect to NP concentration consisting of mean value with variance at each concentration level. (a) Enhancement in iron phosphide-based NFs; (b) Enhancement in iron (II, III) oxide-based NFs; (c) Enhancement in cobalt (II, III) oxide-based NFs.

breakdown voltage is up to 0.0022% concentration and then drops with synthetic ester oil as base fluid. The maximum breakdown voltage is achieved at 0.0022% concentration

TABLE 2. Properties of nanoparticles.

Properties	Iron (II, III) oxide	Cobalt (II, III) oxide	Iron Phosphide [20]
Assay	97% trace metals basis	99.5% trace metals basis	99.5% trace metals basis
Particle size	50-100 nm	<50 nm	50-100 nm
Surface area	>60 m^2/g	40-70 m^2/g	50-80 m^2/g
MP	1538 °C	895 °C	1100 °C
Density (25 °C)	4.8-5.1 g/ml	6.11 g/ml	6.74 g/ml

under the VDE electrode system while maximum enhancement is found in the spherical electrode system. The maximum enhancement of 33.5% is achieved with iron phosphide-based NFs as compared with iron oxide-based NFs.

For cobalt (II, III) oxide-based NFs as shown in Figure 3(c), the breakdown voltage kept increasing with the increase in the NP concentration indicating no saturation point till the range of NP concentration taken in the experiment. The non-achievement of saturation shows that the maximum breakdown strength is above 0.004% NP concentration. Therefore, the maximum enhancement for all cobalt (II, III) oxide NFs is observed at 0.004% as saturation has not been observed. The dissimilarities in trends observed in cobalt oxides NF as compared with iron oxides or iron phosphide NFs are possibly due to the difference in the metallic properties of the elements and size of NPs.

B. RELATIVE PERMITTIVITY

Table 3 represents the average relative permittivities of the prepared nanofluids at different conditions. When compared with the base oil, there has been a significant increase in the relative permittivity for all the types of NFs at the specific value of concentrations. Equation (2) is used to calculate the percentage change in dielectric permittivity ($\Delta\ \in_r\ (\%)$) of NF with each increment in NP concentration.

$$\Delta\ \in_r\ (\%) = \left(\frac{\in_{r\_nf}}{\in_{r\_base\_oil}} - 1\right) * 100 \qquad (2)$$

where, $\in_{r\_nf}$ is the relative permittivity of NF and $\in_{r\_base\_oil}$ is the relative permittivity of base oil.

Figure 4 shows the graphical comparisons of the relative permittivities of three types of NFs at different concentrations for two types of insulating oils. Figure 4(a) shows that percentage change in NFs with base fluids as synthetic ester oil where the maximum percentage change among all three NPs occurs at iron phosphide NP-based NF. Iron phosphide-based NF shows the highest permittivity at 0.003% NP concentration among the three NFs, whereas, cobalt (II, III) oxide shows the least for synthetic ester base oil. The higher value of permittivity signifies more charge accumulation capacity of dielectric materials. Iron phosphide shows maximum charge accumulation capability among all three NPs which results in higher relative permittivity of the NF. Cobalt (II, III) oxide shows less efficiency toward charged particles as compared to other magnetic NPs. The effective relative permittivity of

TABLE 3. Average relative permittivities of prepared nanofluids at different concentrations.

Concentration (w/w%)	Relative permittivity (ϵ_r)					
	Iron Phosphide		Iron (II, III) Oxide		Cobalt (II, III) oxide	
	Synthetic Ester Oil	Natural Ester Oil	Synthetic Ester Oil	Natural Ester Oil	Synthetic Ester Oil	Natural Ester Oil
0	2.697	2.621	2.697	2.621	2.697	2.621
0.0012	2.804	2.645	2.721	2.597	2.721	2.636
0.0022	2.864	2.691	2.808	2.737	2.749	2.658
0.0030	2.883	2.713	2.781	2.703	2.784	2.716
0.0040	2.842	2.719	2.689	2.634	2.673	2.6

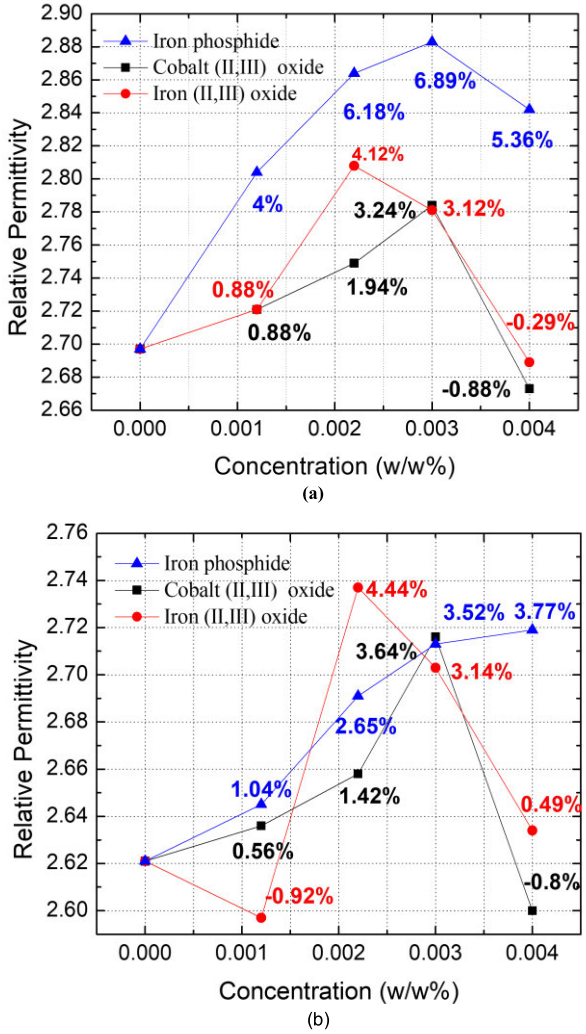

FIGURE 4. (a) Relative permittivity of NFs with synthetic ester oil as a base fluid; (b) Relative permittivity of NFs with natural ester oil as a base fluid.

the NFs depends on the polarization of the molecules present in the solution. When the concentration of the solution is increased the number of particles increase indicating higher polarization than the host fluid. Therefore, the permittivity of prepared NFs increase. However, the permittivity declined due to the unstable nanoparticles in the solution.

The percentage change in relative permittivities of NFs with natural ester as base oil are shown in Figure 4(b). Iron (II, III) oxide-based NF shows the highest relative permittivity at 0.0022% of NP concentration, but its permittivity drops drastically with increasing NP concentration. Whereas iron phosphide-based NF shows a continuous increase in permittivity with increasing NP concentration. On comparing base fluids, the relative permittivity of NF with natural ester oil shows better results as compared to synthetic ester oil. With the increase in NP concentration beyond the saturation point, dielectric properties drastically changed. Iron phosphide-based NF with natural ester oil shows promising results as compared with other prepared NFs.

C. STATISTICAL ANALYSIS

The multiple and lengthy data set of breakdown voltages require the estimation through a probability distribution model since normal distribution provides unclear or erroneously low probability [25]. Weibull distribution is an accepted technique to determine the probability distribution of the breakdown strength. Weibull distributions are employed in many reliability and lifespan evaluations, which is based on the failure of the whole chain due to the presence of a weakest or failed link in it. The results comprise of more than 20 breakdowns for each prepared NFs and base oils. The equation (3) is the 2-parameter Weibull probability density function having shape parameter (k) and scale parameter (c) [26]. The voltage stress limit is governed by these two parameters.

$$f(V) = \frac{dF(V)}{dV} = \frac{k}{c}.\left(\frac{V}{c}\right)^{k-1}.\mathrm{e}^{-\left(\frac{V}{c}\right)^{k}} \tag{3}$$

V, c, and k are voltage (kV), scale factor, and shape factor (dimensionless) respectively. The cumulative distribution function (Weibull function) can be examined using equation (4).

$$F(V) = \int_{o}^{V} f\left(\dot{V}\right) d\dot{V} = 1 - \mathrm{e}^{-\left(\frac{V}{c}\right)^{k}} \tag{4}$$

The shape parameter (k) of Weibull distribution governs the most suitable member in the Weibull distribution family as it determines the Weibull slope (threshold parameter). A greater k value signifies a lesser discreteness of the population. The scale factor assesses the characteristic life of the sample under investigation. The breakdown strength at 63.2% and 1% probability are significant to provide the

TABLE 4. Shape parameter of prepared nanofluids at different concentrations (M-M).

Concentration (w/w%)	Shape Parameter					
	Iron Phosphide		Iron (II, III) Oxide		Cobalt (II, III) oxide	
	Synthetic Ester Oil	Natural Ester Oil	Synthetic Ester Oil	Natural Ester Oil	Synthetic Ester Oil	Natural Ester Oil
0	8.83	12.21	8.83	12.21	8.83	12.21
0.0012	12.22	7.07	17.67	7.85	17.14	12.16
0.0022	9.71	12.26	19.1	12.61	20.39	13.11
0.0030	9.02	10.29	15.36	12.28	11.85	14.28
0.0040	8.7	11.97	14.12	10.95	19.68	11.26

TABLE 5. Shape parameter of prepared nanofluids at different concentrations (S-S).

Concentration (w/w%)	Shape Parameter					
	Iron Phosphide		Iron (II, III) Oxide		Cobalt (II, III) oxide	
	Synthetic Ester Oil	Natural Ester Oil	Synthetic Ester Oil	Natural Ester Oil	Synthetic Ester Oil	Natural Ester Oil
0	5.24	5.5	5.24	5.5	5.24	5.5
0.0012	4.66	5.54	6.21	6.69	6.6	5.56
0.0022	4.88	6.11	7.59	5.16	5.53	5.26
0.0030	5.27	4.92	6.24	5.57	6.11	5.87
0.0040	5.06	5.84	5.35	6.01	5.72	5.44

TABLE 6. Scale parameter of prepared nanofluids at different concentrations (M-M).

Concentration (w/w%)	Scale Parameter					
	Iron Phosphide		Iron (II, III) Oxide		Cobalt (II, III) oxide	
	Synthetic Ester Oil	Natural Ester Oil	Synthetic Ester Oil	Natural Ester Oil	Synthetic Ester Oil	Natural Ester Oil
0	68.62	64.79	68.62	64.79	68.62	64.79
0.0012	69.57	67.9	71.9	68.89	67.08	65.43
0.0022	82.1	73.29	80.58	69.16	68.01	69.61
0.0030	72.06	75.89	69.27	70.12	72.79	74.75
0.0040	60.62	77.36	64.75	72.38	76.73	81.34

detailed of failures possibility in NFs and it can be easily determined using two-parameter Weibull distribution for the voltage dataset.

In this experiment, Weibull analysis is performed to visualize the breakdown probability of prepared NFs as the average breakdown characteristics are not deterministic. Figure 3 shows the enhancement of the breakdown voltage whose value is taken as the average. Whereas, during the Weibull analysis, each reading of the breakdown voltage for each prepared NFs is taken into consideration, and accordingly, points on the graphs have been plotted. While recording the breakdown voltage of the NFs, the values of breakdown voltage are different whose illustrations are provided by the Weibull distribution curve with the breakdown probability. Therefore, by this analysis, the probability of breakdown of NFs at different voltage is analyzed. The shape parameter for VDE electrode and sphere electrode configurations are estimated and tabulated in Table 4 and 5, respectively. The Scale parameter for VDE electrode and sphere electrode configurations are estimated and tabulated in Table 6, and 7, respectively. Further, the breakdown strength at 63.2% and 1% probability are tabulated in Table 8, 9, and 10 for iron phosphide, cobalt (II, III) oxide, and iron (II, III) oxide-based NFs respectively to analyze probability distribution for each prepared NF.

For the graphical analysis of Weibull distribution, Figure 5 represents the Weibull Probability Distribution of failure (%) with respect to breakdown voltage (kV) for different NPs in synthetic ester oil-based NFs. Both the electrode configurations have been plotted for NF with different NP concentrations. Iron phosphide, cobalt (II, III) oxide, and iron (II, III) oxide-based NFs are represented in Figure 5(a), (b) and, (c)

TABLE 7. Scale parameter of prepared nanofluids at different concentrations (S-S).

Concentration (w/w%)	Scale Parameter					
	Iron Phosphide		Iron (II, III) Oxide		Cobalt (II, III) oxide	
	Synthetic Ester Oil	Natural Ester Oil	Synthetic Ester Oil	Natural Ester Oil	Synthetic Ester Oil	Natural Ester Oil
0	37.62	34.42	37.62	34.42	37.62	34.42
0.0012	42.74	37.68	42.08	37.48	38.48	37.33
0.0022	49.65	39.98	48.18	39.19	39.84	40.31
0.0030	41.56	42.57	43.30	42.98	42.24	42.14
0.0040	36.54	45.78	36.78	44.77	43.47	47.05

TABLE 8. Different breakdown voltage probabilities of iron phosphide based nanofluids.

Carrier Liquid	Electrode Structure	Breakdown Probabilities (%)	Iron Phosphide				
			Breakdown Voltage (kV)				
			0%	0.0012%	0.0022%	0.003%	0.004%
Synthetic Ester Oil	M-M	1	40.76	47.74	51.11	43.27	35.72
		63.2	68.42	69.57	82.1	72.07	60.63
	S-S	1	15.65	15.92	19.35	17.35	14.71
		63.2	37.62	42.74	49.65	41.56	36.55
Natural Ester Oil	M-M	1	44.46	35.44	50.35	48.48	52.68
		63.2	64.79	67.9	73.29	75.89	77.36
	S-S	1	14.93	16.42	18.83	16.71	20.82
		63.2	34.42	37.68	39.98	42.57	45.78

TABLE 9. Different breakdown voltage probabilities of cobalt (II, III) oxide based nanofluids.

Carrier Liquid	Electrode Structure	Breakdown Probabilities (%)	Cobalt (II, III) Oxide				
			Breakdown Voltage (kV)				
			0%	0.0012%	0.0022%	0.003%	0.004%
Synthetic Ester Oil	M-M	1	40.76	51.3	54.27	49.36	58.21
		63.2	68.42	67.08	68	78.79	60.73
	S-S	1	15.65	19.18	17.34	19.91	19.45
		63.2	37.62	38.48	39.84	42.24	43.47
Natural Ester Oil	M-M	1	44.46	44.82	49.02	54.16	54.6
		63.2	64.79	65.43	69.61	74.75	81.34
	S-S	1	14.93	16.32	16.82	19.26	20.22
		63.2	34.42	37.33	40.31	42.14	47.05

TABLE 10. Different breakdown voltage probabilities of iron (II, III) oxide based nanofluids.

Carrier Liquid	Electrode Structure	Breakdown Probabilities (%)	Iron (II, III) oxide				
			Breakdown Voltage (KV)				
			0%	0.0012%	0.0022%	0.003%	0.004%
Synthetic Ester Oil	M-M	1	40.76	55.41	63.33	51.35	46.74
		63.2	68.42	71.9	80.58	69.27	64.74
	S-S	1	15.65	20.06	26.28	20.72	15.57
		63.2	37.62	42.08	48.18	43.3	36.78
Natural Ester Oil	M-M	1	44.46	38.34	48.02	48.2	47.54
		63.2	64.79	68.89	69.16	70.12	72.38
	S-S	1	14.93	18.84	16.08	18.83	20.83
		63.2	34.42	37.48	39.19	42.98	44.77

respectively. Among all iron phosphide-based NF prepared, the maximum breakdown voltage at 63.2% was 82.1 kV at 0.0022% concentration for synthetic ester oil in the M-M electrode configuration. Among all iron oxide-based NFs prepared, the maximum breakdown voltage at 63.2% was 80.58 kV at 0.0022% concentration for synthetic ester oil in the M-M electrode configuration.

Figure 6 shows the Weibull Probability Distribution of failure (%) with respect to breakdown voltage (kV) for different NPs in natural ester oil-based NFs. Figure 6(a), (b), and (c) represent the iron phosphide, cobalt (II, III) oxide, and iron (II, III) oxide NP-based NF respectively with similar NP concentration range. Among all cobalt oxide-based NF prepared, the maximum breakdown voltage at 63.2% was 81.34 kV

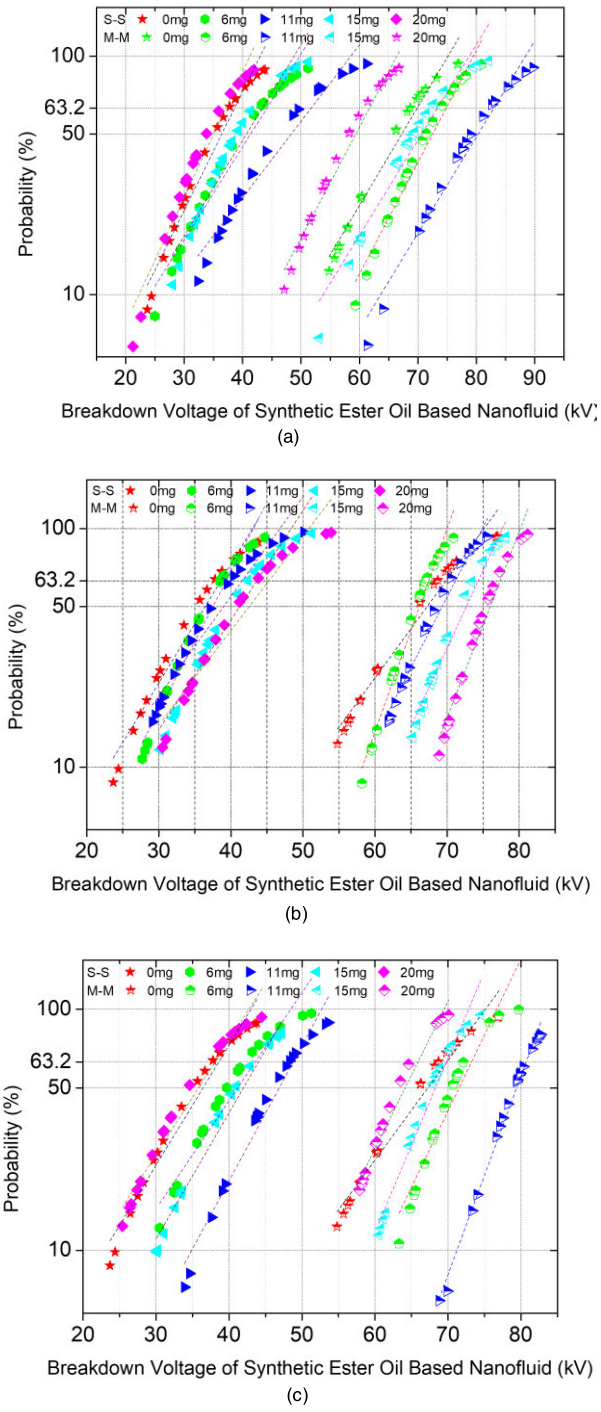

FIGURE 5. The Weibull probability distributions of the breakdown of NFs with synthetic ester oil as a base fluid (a) Iron Phosphide-based NFs; (b) Cobalt (II, III) oxide-based NFs; (c) Iron (II, III) oxide-based NFs.

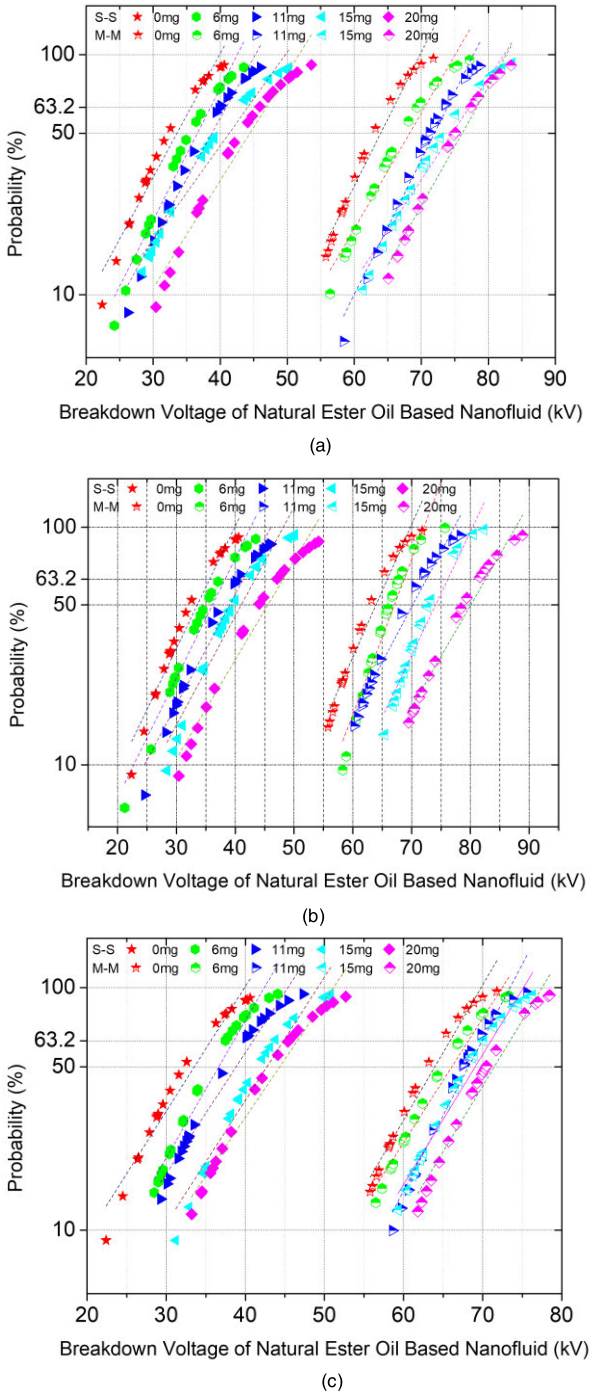

FIGURE 6. The Weibull probability distributions of breakdown of NFs with natural ester oil as a base fluid. (a) Iron Phosphide based NFs; (b) Cobalt (II, III) oxide-based NFs; (c) Iron (II, III) oxide-based NFs.

at 0.004% concentration for natural ester oil in the M-M electrode configuration.

The research on iron phosphide-based NFs with natural ester oil shows its applicability as dielectric fluids in the futuristic transformer oil. The use of vegetable oil makes it more eco-friendly as compared to conventional mineral oil. However, there are several factors, which must be taken into consideration while choosing the NFs. Factors such as the effect of temperature, humidity, stability, and aging of NFs are among important considerations for selection. These factors need to be evaluated and the optimization of NP concentration can be investigated in future work.

IV. CONCLUSION

In this article, a comparative study on the effects of NPs in synthetic ester oil and natural ester oil has been performed

experimentally. The different electrode configurations have been used to determine the breakdown voltage and relative permittivity. The novel iron phosphide NPs have been prepared and dispersed uniformly in ester oils by the two-step method. Breakdown strength and relative permittivity of the iron phosphide-based NFs are compared with the other NFs in terms of NP types and their concentrations. Further, Weibull probability distribution curves have been plotted and the tables have been formulated showing the breakdown voltages at 1% and 63.2% probability.

All the NFs show enhancements in their breakdown strength, which are requirements of the insulating oil. The maximum breakdown strength is achieved with iron phosphide-based NF at a specific concentration of NPs. The evaluation of iron phosphide-based NFs further requires life evaluation and stability, which can be improved to make commercially competed. Future experimental analyses such as moisture effect, temperature, resistivity, acidity, viscosity, etc. need to be performed to determine the potential of iron phosphide-based NFs to be used as the transformer oil.

APPENDIX

A. BACKGROUND OF NANOFLUID

Nanofluid (NF) is defined as a colloidal solution developed with the stable dispersion of nanoparticles (NPs) in the base oil using stabilizing agents that enhance or add the characteristics in the prepared colloid [27]. Extensive research activity on NFs has been devoted over the last decade, as the addition of a few nano-sized particles in the medium not just strengthen the existing characteristics of fluid but also introduce new properties that enhance its applicability [28], [29]. Recently, many techniques have been employed to improve the dielectric property of transformer oil with the addition of NPs to improve quality and enhance the dielectric fluid [30]. The enhanced dielectric and thermal properties of NFs as compared to the corresponding base liquid insulation are the reason for its futuristic applications in power transformers.

NFs are categorized into different categories based on the NP types: ceramic. pure metallic, non- metallic, oxide, carbide, alloy, nano-scaled liquid droplets, and carbon-based NFs [31]. NFs applications are continuously developed in different areas of engineering. Initially, the magnetic NFs were fabricated using iron oxide which revealed enrichment in the dielectric as well as thermal strength [32]. The nature of insulating liquid can be polar or non-polar and both showing improvements in their properties with the dispersion of NPs at the optimum concentrations [33]. Various NPs including magnetic, metallic, semi-conductive, and insulative nature are used with different insulating mediums to improve the quality of insulants. The other metal oxide NPs-based NFs like TiO_2 [19], SiO_2, Al_2O_3, CuO, ZnO, MgO [34] show enhancement in dielectric properties.

The magnetic NF is a colloid that constitutes magnetic NPs dispersed in a carrier liquid with the help of a surfactant as shown in Figure 7 [9]. Magnetic NFs have shown some promising results in dielectric and thermal applications,

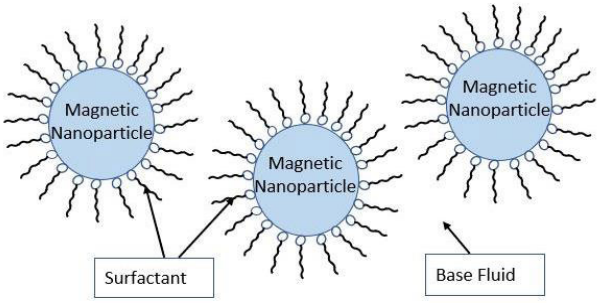

FIGURE 7. Dispersion of magnetic nanoparticles in the dielectric fluid [9].

which promotes further research. Possessing the magnetic property, it is feasible to regulate the fluid flow, heat transfer, and particle movement by the application of the magnetic field. This exceptional property of magnetic NFs is utilized in different fields like thermal engineering, electronics, bio-engineering, etc. NFs as the dielectric fluid usually comprise of mineral oil, synthetic oil, and vegetable oil as base fluid to provide high dielectric strength. The surfactants cover the NP's active surface to minimize the possibility of coagulation. This process helps to uniformly distribute the NPs into the solution and improve the stability and heat transfer capability [19].

B. INFLUENCE OF SURFACE CHARGING OF NANOPARTICLES IN NANOFLUID

The polarizing characteristic of the magnetic NPs results in the greater permittivity of NPs than the surrounding medium indicating instantaneous surface charging. The relaxed magnetic NPs in the fluid behaves as the perfect conductors due to extremely short relaxation time and the electric field line converges on the NPs. Therefore, the uniform electric field distribution is not appearing in NFs due to the presence of NPs. The difference in the electric characteristics of NPs and fluid causes non-uniform field which is given by the below equations (5) & (6) [35]:

$$E_r(r,\theta) = E_0 cos\theta \left[1 + \left\{\left(\frac{d_{np}^3}{4r^3}\right)\left(\frac{\varepsilon_{np}-\varepsilon_f}{\varepsilon_{np}+2\varepsilon_f}\right)e^{-t/\tau}\right\} + \left\{\left(\frac{d_{np}^3}{4r^3}\right)\left(\frac{\sigma_{np}-\sigma_f}{\sigma_{np}+2\sigma_f}\right)(1-e^{-t/\tau})\right\}\right] \quad (5)$$

$$E_\theta(r,\theta) = E_0 sin\theta \left[-1 + \left\{\left(\frac{d_{np}^3}{8r^3}\right)\left(\frac{\varepsilon_{np}-\varepsilon_f}{\varepsilon_{np}+2\varepsilon_f}\right)e^{-t/\tau}\right\} + \left\{\left(\frac{d_{np}^3}{4r^3}\right)\left(\frac{\sigma_{np}-\sigma_f}{\sigma_{np}+2\sigma_f}\right)(1-e^{-t/\tau})\right\}\right] \quad (6)$$

where, E_0 is the Electric field; (r, θ, z) is the cylindrical coordinates at the time (t), ε is the absolute permittivity, τ is the charge relaxation time, σ is electrical conductivity, NP – NPs, f is the fluid. The calculation of charge relaxation time is given by [36]:

$$\tau = \frac{2\varepsilon_f + \varepsilon_{np}}{2\sigma_f + \sigma_{np}} \quad (7)$$

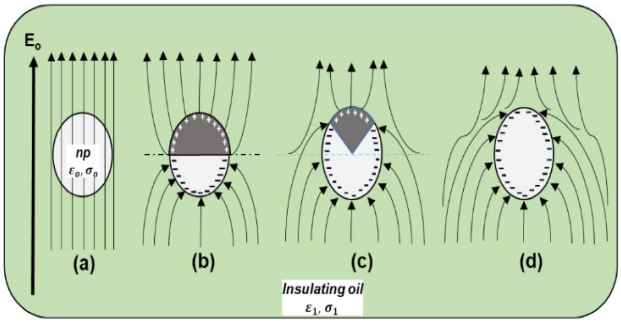

FIGURE 8. Electric displacement and polarization of insulating medium due to the presence of conductive NPs under electric field [30].

Generally, the time scale for streamer build-up in the stressed oil is between 10^{-10}s and 10^{-6}s. The NP inside the insulating oils is shown in Figure 8 [30]. Figure 8(a) shows the property of absorbing the ions when oil is undergoing the ionization phase giving lesser freedom for the current path. The lesser probability of breakdown at lower voltage thereby giving inflated electrical stress-bearing capability as shown in Figure 8(b) and 8(c). The limited absorption capability of the NFs, when the absorption capability reaches the saturation point as shown in Figure 8(d), the absorption of the electrons is blocked, and breakdown takes place. When the concentration of NPs is raised, the absorption capability of the NFs is elevated leading to a higher breakdown, when compared to the lower concentration. This indicates that when the concentration of the NPs is raised, there is an enhancement in the dielectric breakdown.

The finite element method (FEM) is widely used in the visualization of the electric stress in power transformer insulation [37]. Thus, it becomes widely used and very informative in determining the effect of the electric field on NFs [38], [39]. In [38], the author explained the effect of NPs in the transformer oil due to different dielectric properties creating a non-uniform electric field. In [39], the author explains low electric field stress near NP resulting in a higher breakdown voltage of NFs. With a high surface current density of NPs, easier streamer penetration happens in natural ester. The impact of NPs on streamer development is proportional to the delay in the breakdown of insulation. In [35], the author performed the experiment showing the linear increase in the negative ion charge density distribution from the ionization zone to the needle electrode tip for pure transformer oil under needle-sphere electrode system. Practically, charging decays after reaching the saturation point in case of NFs which is a contradiction to the expected linear charge density distribution. The ionization of the NF results in the liberation of both the positive as well as negatively charged particles with the rapid increment in negatively charged particle density. The positively charged particles are practically immobile due to the higher weight as compared to the electrons. This is the reason that the NPs come into contact with the electrons more than the positively charged ions resulting in the negatively charged nanostructure, thereby absorbing electrons. As the NPs are crowded by negative charge, they repel the movements of the electrons between the electrodes resulting in the weakening charge absorption effectiveness, and lesser possibility of the nanostructure to reach the saturation point. Nanoparticles charge holding capacity (Q_s) can be governed by the equation 8 [38].

$$Q_s = \begin{cases} -12\pi\varepsilon_1 E_o R^2 & \textit{conductive particle} \\ -12\pi\varepsilon_1 E_o R^2 \dfrac{\varepsilon_2}{2\varepsilon_1 + \varepsilon_2} & \textit{dielectric particle} \end{cases} \tag{8}$$

where, E_o, R, ε_1, and ε_2 are applied electric field (V/m), the radius of particle (m), permittivity of oil, and permittivity of particle respectively. It is clear from Eq. (8), the NPs with higher permittivity exhibits better charge holding capacity due to increased trapping of charges. More charges at low NF concentration results in higher trapping performance, and higher breakdown strength. Also, the charge directly depends on the radius (size) of NP. Therefore, the NP having a lower size has a lower charge than a higher size NP. This means that for the same NP under the same concentration but different NP size, the number of NPs is higher for the lower NP size. Due to this, it has been observed that at the same concentration, there is an increment in the total saturation charge for the lower NP size than higher NP size. Therefore, the maximum breakdown strength is higher for lower sized of NP at the same concentration.

C. INFLUENCE OF NANOPARTICLES ON THE RELATIVE PERMITTIVITY OF NANOFLUID

There are different methods proposed to find the influence of nanoparticles on the relative permittivity of NFs as mentioned in [40]. The type of NP plays an important role in the overall relative permittivity of NFs. Maxwell-Garnett equation for the calculation of the relative permittivity of the mixed dielectric (here NF) is [41]:

$$\tau = \frac{\varepsilon_{r,n} - \varepsilon_{r1}}{\varepsilon_{r,n} + 2\varepsilon_{r1}} = \varphi \frac{\varepsilon_{r2} - \varepsilon_{r1}}{\varepsilon_{r2} + 2\varepsilon_{r1}} \tag{9}$$

where, ε_{r1} and, ε_{r2} are relative permittivities of the host fluid and spherical NP respectively. $\varepsilon_{r,n,}$ and φ are the relative permittivity of the NF and the spherical NP volumetric concentration respectively. In the case of transformer oil-based NFs, the NP contribution can be considered to be negligible due to very low volumetric concentration, resulting in the negligible effect of relative permittivity by NP. To consider the effect of NP on relative permittivity, the polarization model is proposed in which both the host fluid molecules and NP gets polarized. Polarization happens in the form of fluid polarization, inner NP polarization as shown in Figure 9 [40]. Also, polarization takes place in the form of orientational polarization of charged NP when considered as a polar molecule. Clausius-Mossotti expressed the relative permittivity of transformer oil-based NF ($\varepsilon_{r,n}$) considering all three types of polarization by the equation [41]:

$$\frac{\varepsilon_{r,n} - 1}{\varepsilon_{r,n} + 2} = \frac{1}{3\varepsilon_0}(N_1\alpha_1 + N_2\alpha_2 + N_2\alpha_3) \tag{10}$$

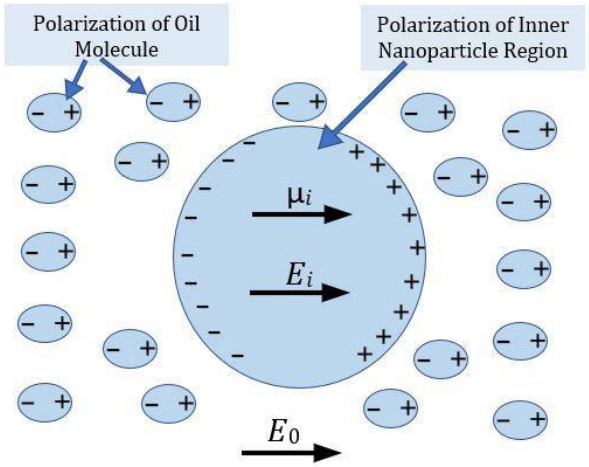

FIGURE 9. Polarization of oil molecule and NP in TF oil-based NFs [40].

where, α_1, α_2, and α_3 are polarizability of transformer oil molecule, NP due to inner polarization, and orientational polarization of charged NP when considered as polar molecule respectively. N_1 and N_2 are per unit volume of the number of molecules of transformer oil and NP respectively.

Clausius-Mossotti equation can be further deduced to the following equation [40]:

$$\frac{\varepsilon_{r,n}-1}{\varepsilon_{r,n}+2}=\frac{\varepsilon_1-1}{\varepsilon_1+2}+\frac{\varphi}{3}(\varepsilon_2-1)+\frac{\varphi}{3kT}\pi\varepsilon_0 a^3 E_0^2\left(\frac{\varepsilon_{r2}-\varepsilon_{r1}}{2\varepsilon_1+\varepsilon_{r2}}\right)^2 \quad (11)$$

where, k and T are Boltzmann constant and thermodynamic temperature ($^\circ K$) respectively. The inference of the polarization of the NF is that upon the increase in the NP concentration increases the permittivity of the NF. However, the experimental result of the relative permittivity of NFs may not be linear [42].

REFERENCES

[1] B. Du, X. Li, and M. Xiao, "High thermal conductivity transformer oil filled with BN nanoparticles," *IEEE Trans. Dielectr. Electr. Insul.*, vol. 22, no. 2, pp. 851–858, Apr. 2015.

[2] D. K. Devendiran and V. A. Amirtham, "A review on preparation, characterization, properties and applications of nanofluids," *Renew. Sustain. Energy Rev.*, vol. 60, pp. 21–40, Jul. 2016.

[3] A. R. P. R. Thirugnanam, W. I. M. Siluvairaj, and R. Karthik, "Performance studies on dielectric and physical properties of eco-friendly based natural ester oils using semi-conductive nanocomposites for power transformer application," *IET Sci., Meas. Technol.*, vol. 12, no. 3, pp. 323–327, May 2018.

[4] M. Rafiq, D. Khan, and M. Ali, "Dielectric properties of transformer oil based silica nanofluids," in *Proc. Power Gener. Syst. Renew. Energy Technol.*, Jun. 2015, pp. 1–3.

[5] S. U. S. Choi, "Nanofluids: From vision to reality through research," *J. Heat Transf.*, vol. 131, no. 3, Mar. 2009, Art. no. 033106.

[6] S. K. Sharma and S. M. Gupta, "Preparation and evaluation of stable nanofluids for heat transfer application: A review," *Experim. Thermal Fluid Sci.*, vol. 79, pp. 202–212, Dec. 2016.

[7] B. X. Du and X. L. Li, "Dielectric and thermal characteristics of vegetable oil filled with BN nanoparticles," *IEEE Trans. Dielectr. Electr. Insul.*, vol. 24, no. 2, pp. 956–963, Apr. 2017.

[8] M. Rajnak, Z. Wu, B. Dolnik, K. Paulovicova, J. Tothova, R. Cimbala, J. Kurimský, P. Kopcansky, B. Sunden, L. Wadsö, and M. Timko, "Magnetic field effect on thermal, dielectric, and viscous properties of a transformer oil-based magnetic nanofluid," *Energies*, vol. 12, no. 23, pp. 1–11, 2019.

[9] Y. Lv, M. Rafiq, C. Li, and B. Shan, "Study of dielectric breakdown performance of transformer oil based magnetic nanofluids," *Energies*, vol. 10, no. 7, p. 1025, Jul. 2017.

[10] M. Rafiq, C. Li, Y. Lv, K. Yi, and Q. Sun, "Breakdown characteristics of mineral oil based magnetic nanofluids," in *Proc. IEEE Int. Conf. High Volt. Eng. Appl. (ICHVE)*, Sep. 2016, pp. 10–13.

[11] J.-C. Lee and W.-Y. Kim, "Experimental study on the dielectric breakdown voltage of the insulating oil mixed with magnetic nanoparticles," *Phys. Procedia*, vol. 32, pp. 327–334, Aug. 2012.

[12] Q. Wang, M. Rafiq, Y. Lv, C. Li, and K. Yi, "Preparation of three types of transformer oil-based nanofluids and comparative study on the effect of nanoparticle concentrations on insulating property of transformer oil," *J. Nanotechnol.*, vol. 2016, pp. 1–6, Jan. 2016.

[13] G. D. Peppas, M. G. Danikas, A. Bakandritsos, V. P. Charalampakos, E. C. Pyrgioti, and I. F. Gonos, "Statistical investigation of AC breakdown voltage of nanofluids compared with mineral and natural ester oil," *IET Sci., Meas. Technol.*, vol. 10, no. 6, pp. 644–652, Sep. 2016.

[14] F. Ahmad, A. A. Khan, Q. Khan, and M. R. Hussain, "State-of-art in nano-based dielectric oil: A review," *IEEE Access*, vol. 7, pp. 13396–13410, 2019.

[15] A. M. Abd-Elhady, M. E. Ibrahim, T. A. Taha, and M. A. Izzularab, "Effect of temperature on AC breakdown voltage of nanofilled transformer oil," *IET Sci., Meas. Technol.*, vol. 12, no. 1, pp. 138–144, Jan. 2018.

[16] A. Katiyar, P. Dhar, T. Nandi, and S. K. Das, "Effects of nanostructure permittivity and dimensions on the increased dielectric strength of nano insulating oils," *Colloids Surf. A, Physicochemical Eng. Aspects*, vol. 509, pp. 235–243, Nov. 2016.

[17] M. Maharana, M. M. Bordeori, S. K. Nayak, and N. Sahoo, "Nanofluid-based transformer oil: Effect of ageing on thermal, electrical and physico-chemical properties," *IET Sci., Meas. Technol.*, vol. 12, no. 7, pp. 878–885, Oct. 2018.

[18] Y. Hou, Z. Zhang, and J. Zhang, "Significantly improved breakdown performances of propylene carbonate-based nano-fluids," *Micro Nano Lett.*, vol. 11, no. 9, pp. 490–493, Sep. 2016.

[19] E. G. Atiya, D.-E.-A. Mansour, R. M. Khattab, and A. M. Azmy, "Dispersion behavior and breakdown strength of transformer oil filled with TiO_2 nanoparticles," *IEEE Trans. Dielectr. Electr. Insul.*, vol. 22, no. 5, pp. 2463–2472, Oct. 2015.

[20] Q. Khan, R. Hussain, and A. A. Khan, "Dielectric characterisation of Fe_3P nanoparticles based ester oil," *IET Nanodielectrics*, vol. 1, no. 4, pp. 132–136, Dec. 2018.

[21] N. A. Mohamad, N. Azis, J. Jasni, M. Z. A. Ab Kadir, R. Yunus, and Z. Yaakub, "Impact of Fe_3O_4, CuO and Al_2O_3 on the AC breakdown voltage of palm oil and coconut oil in the presence of CTAB," *Energies*, vol. 12, no. 9, p. 1605, Apr. 2019.

[22] G. D. Peppas, V. P. Charalampakos, E. C. Pyrgioti, A. Bakandritsos, A. D. Polykrati, and I. F. Gonos, "A study on the breakdown characteristics of natural ester based nanofluids with magnetic iron oxide and SiO_2 Nanoparticles," in *Proc. IEEE Int. Conf. High Voltage Eng. Appl. (ICHVE)*, Sep. 2018, pp. 1–4.

[23] Y. Mohammadfam, S. Zeinali Heris, and L. Khazini, "Experimental investigation of Fe_3O_4/hydraulic oil magnetic nanofluids rheological properties and performance in the presence of magnetic field," *Tribol. Int.*, vol. 142, Feb. 2020, Art. no. 105995.

[24] M. R. Hussain, "Effect of magneto-nanofluids on breakdown characteristics of insulating oil," M.Tech dissertation, Dept. Elect. Eng., Aligarh Muslim Univ., Aligarh, India, 2017.

[25] U. Khaled and A. Beroual, "AC dielectric strength of synthetic ester-based Fe_3O_4, Al_2O_3 and SiO_2 nanofluids—Conformity with normal and weibull distributions," *IEEE Trans. Dielectr. Electr. Insul.*, vol. 26, no. 2, pp. 625–633, Apr. 2019.

[26] A. Azad, M. Rasul, and T. Yusaf, "Statistical diagnosis of the best weibull methods for wind power assessment for agricultural applications," *Energies*, vol. 7, no. 5, pp. 3056–3085, May 2014.

[27] O. Mahian, L. Kolsi, M. Amani, P. Estellé, G. Ahmadi, C. Kleinstreuer, J. S. Marshall, M. Siavashi, R. A. Taylor, H. Niazmand, S. Wongwises, T. Hayat, A. Kolanjiyil, A. Kasaeian, and I. Pop, "Recent advances in modeling and simulation of nanofluid flows-part I: Fundamentals and theory," *Phys. Rep.*, vol. 790, pp. 1–48, Feb. 2019.

[28] G. Shukla and H. Aiyer, "Thermal conductivity enhancement of transformer oil using functionalized nanodiamonds," *IEEE Trans. Dielectr. Electr. Insul.*, vol. 22, no. 4, pp. 2185–2190, Aug. 2015.
[29] W. Sima, H. Guo, P. Sun, Q. Chen, and H. Song, "Effect of nanoparticles on impulse breakdown performance of propylene carbonate based on modified kerr electro-optic measurements," *IEEE Trans. Dielectr. Electr. Insul.*, vol. 24, no. 5, pp. 2784–2790, Oct. 2017.
[30] A. Thabet, M. Allam, and S. A. Shaaban, "Investigation on enhancing breakdown voltages of transformer oil nanofluids using multi-nanoparticles technique," *IET Gener., Transmiss. Distrib.*, vol. 12, no. 5, pp. 1171–1176, Mar. 2018.
[31] A. K. Sharma, A. K. Tiwari, and A. R. Dixit, "Rheological behaviour of nanofluids: A review," *Renew. Sustain. Energy Rev.*, vol. 53, pp. 779–791, Jan. 2016.
[32] V. Segal, A. Rabinovich, D. Nattrass, K. Raj, and A. Nunes, "Experimental study of magnetic colloidal fluids behavior in power transformers," *J. Magn. Magn. Mater.*, vols. 215–216, pp. 513–515, Jun. 2000.
[33] S. Bucko, M. Krchňák, R. Cimbala, L. Kruzelak, and J. Zbojovsky, "Abrasive properties of transformer oil-based magnetic nanofluid," in *Proc. 19th Int. Sci. Conf. Electr. Power Eng. (EPE)*, May 2018, pp. 1–4.
[34] P. Thomas, "Breakdown voltage and gassing tendency of synthetic esters based MgO nanofluids," in *Proc. IEEE 4th Int. Conf. Condition Assessment Techn. Electr. Syst. (CATCON)*, Chennai, India, Nov. 2019, pp. 1–3.
[35] J. G. Hwang, M. Zahn, F. M. O'Sullivan, L. A. A. Pettersson, O. Hjortstam, and R. Liu, "Effects of nanoparticle charging on streamer development in transformer oil-based nanofluids," *J. Appl. Phys.*, vol. 107, no. 1, Jan. 2010, Art. no. 014310.
[36] L. Vékás, D. Bica, and M. V. Avdeev, "Magnetic nanoparticles and concentrated magnetic nanofluids: Synthesis, properties and some applications," *China Particuol.*, vol. 5, nos. 1–2, pp. 43–49, Feb. 2007.
[37] M. R. Hussain and S. S. Refaat, "Dielectric behaviour of defects in power transformer insulation using finite element method," in *Proc. 2nd Int. Conf. Smart Grid Renew. Energy (SGRE)*, Nov. 2019, pp. 1–6.
[38] A. M. Samy, M. E. Ibrahim, A. M. Abd-Elhady, and M. A. Izzularab, "On electric field distortion for breakdown mechanism of nanofilled transformer oil," *Int. J. Electr. Power Energy Syst.*, vol. 117, no. Aug. 2019, pp. 1–7, 2020.
[39] N. A. Sabiha, S. S. M. Ghoneim, and M. M. Hessien, "Breakdown performance of transformer oil in the presence of single-phase nanocrystalline ZnO and nano-partial substitution," *IET Sci., Meas. Technol.*, vol. 13, no. 5, pp. 737–745, Jul. 2019.
[40] J. Miao, M. Dong, M. Ren, X. Wu, L. Shen, and H. Wang, "Effect of nanoparticle polarization on relative permittivity of transformer oil-based nanofluids," *J. Appl. Phys.*, vol. 113, no. 20, pp. 1–6, 2013.
[41] S. O. Kasap, *Principles of Electronic Materials and Devices*. New York, NY, USA: McGraw-Hill, 2006.
[42] A. H. Aref, A. A. Entezami, H. Erfan-Niya, and E. Zaminpayma, "Thermophysical properties of paraffin-based electrically insulating nanofluids containing modified graphene oxide," *J. Mater. Sci.*, vol. 52, no. 5, pp. 2642–2660, Mar. 2017.

MD RASHID HUSSAIN (Graduate Student Member, IEEE) received the Bachelor of Technology and Master of Technology degrees in electrical engineering from Aligarh Muslim University, with the specialization in high voltage and insulation. He is currently working as a Research Associate with Texas A&M University, Qatar. His main research interests include partial discharge analysis, nanofluids, condition monitoring of electric and electronic equipment, high-voltage measurement and insulation development, and nano-dielectrics, finite element analysis, and biomedical engineering. He has published some research articles in his relevant field.

QASIM KHAN (Graduate Student Member, IEEE) received the B.S. degree in electrical engineering and the M.S. degree in electrical engineering with specialization in high voltage and insulation engineering from Aligarh Muslim University, India, in 2012 and 2015, respectively. He is currently pursuing the Ph.D. degree with Texas A&M University, College Station, TX, USA. He has worked as a Research Fellow with AMU, India, for three years. He joined the EMPE Laboratory, in fall 2019. He is also a member of the Smart Grid Center–Extension in Qatar (SGC-Q). His current research interests include condition monitoring of power equipment, partial discharge analysis, finite element modeling, and nanodielectric.

ASFAR ALI KHAN (Member, IEEE) received the B.Sc. (Engg.), M.Tech., and Ph.D. degrees from Aligarh Muslim University, Aligarh, India. He is currently a Professor with the Department of Electrical Engineering, Aligarh Muslim University. He has more than 21 years of teaching experience. He has experience in the field of condition assessment, high-voltage engineering, automation technology, and partial discharges. He has performed a number of electrical failure investigation studies on insulators. He has presented a number of technical and scientific papers at international conferences and seminars. His research interests include high-voltage engineering, insulation design and condition monitoring, nano dielectrics, power systems, and stability studies.

SHADY S. REFAAT (Senior Member, IEEE) received the B.A.Sc., M.A.Sc., and Ph.D. degrees in electrical engineering from Cairo University, Giza, Egypt, in 2002, 2007, and 2013, respectively. He has worked in the industry for more than 12 years as the Engineering Team Leader, a Senior Electrical Engineer, and an Electrical Design Engineer on various electrical engineering projects. He is currently an Associate Research Scientist with the Department of Electrical and Computer Engineering, Texas A&M University, Qatar. He has published more than 105 journal and conference papers. His research interests include electrical machines, power systems, smart grid, big data, energy management systems, reliability of power grids and electric machinery, fault detection, and condition monitoring and development of fault-tolerant systems. He has also participated and leads several scientific projects over the last eight years. He has successfully realized many potential research projects. He is a member of The Institution of Engineering and Technology (IET) and the Smart Grid Center–Extension in Qatar (SGC-Q).

HAITHAM ABU-RUB (Fellow, IEEE) received the Ph.D. degrees. He is currently a Full Professor. He has research and teaching experience at many universities in many countries, including Poland, Palestine, USA, Germany, and Qatar. Since 2006, he has been with Texas A&M University, Qatar. He has served for five years as the Chair of the Electrical and Computer Engineering Program, Texas A&M University, where he is also serving as the Managing Director of the Smart Grid Center. His main research interests include power electronic converters, renewable energy, electric drives, and smart grid. He has published more than 400 journal and conference papers, five books, and six book chapters. He has supervised many research projects on smart grid, power electronics converters, and renewable energy systems. He was a recipient of many national and international awards and recognitions. He was also a recipient of the American Fulbright Scholarship and the German Alexander von Humboldt Fellowship.